HYGROMORPHIC SCALES FOR USE IN WATER FROM MORNING DEW AND ELEMENTARY MODEL OF HYDROGEL EXPANSION PROPERTIES

A THESIS SUBMITTED TO THE

FACULTY OF THE GRADUATE SCHOOL OF

THE UNIVERSITY OF COLORADO

IN PARTIAL FULFILLMENT OF THE REQUIREMENTS

FOR THE DEGREE, OF

MASTER'S OF SCIENCE

DEPARTMENT OF MATERIALS SCIENCE AND ENGINEERING

Nate Margolis
March 2017

This thesis entitled:
Hygromorphic Scales for Use in Water Collection from Morning Dew
And an Elementary Model of Hydrogel Expansion Properties
Written by Nate Margolis
Has Been Approved for the Department of Materials Science and Engineering

Prof. Franck Vernerey

Prof. Yunping Xi

Prof. Rong Long

Date:_______________

The final copy of this thesis has been examined by the signatories, and we find that both the content and the form meet the acceptable presentation standards of scholarly work in the above-mentioned discipline.

Abstract

Margolis, Nate (M.S., Materials Science and Engineering)
Hygromorphic Scales For Use in Water Collection From Morning Dew and an Elementary Model of Hydrogel Expansion Properties
Thesis Directed by Professor Franck Vernerey

Secure access to water is a growing problem in the world today. Millions of people do not have contact with fresh or clean water for drinking. Consuming dirty water leads to many illnesses and deaths every year. When water is scarce people are less likely to follow basic hygiene which also adds to the problem of sickness from water. Currently most of the population gets their water from run-off such as rivers, lakes and other fresh water bodies. Aquafers can also provide water, however, once they do not replenish themselves so once they are empty they will no longer provide a fresh water source.

This is a serious problem because the population has grown to 7 billion people and only 2% of the world's water is fresh water. Of this, most the fresh water is locked in the polar ice caps. This leaves only .77% of the available fresh water accessible for human use. While wealthy countries may not feel this burden due to their infrastructure. Impoverish countries will feel the full burden of a lack of water. This has led to a growing number of water conflicts over the years some of which have resulted in human deaths.

There are several ways that people can collect water from the atmosphere such as collecting rain water or using a solar still to evaporate water out of an undrinkable source. In parts of the world where fog is prevalent, meshes have been used to collect the moisture from the air. However, these systems only work where the environment allows for it. In some places in the world, the only amount of water may come from morning dew. Certain places receive more water from morning dew than they do from annual precipitation.

By studying nature, a novel water collection device was developed, tested and modeled. The model is compared to the test data to see the ways in which the device can be optimized. This could be used to help alleviate the growing problems of water shortages in specific parts of the world. The model and device design shows promising data but still has room for improvement. Potential changes for improved performance are explored.

Acknowledgements

I would like to thank my advisor Frank Vernerey for being so helpful and guiding me through the process of joining the research group and always being there for help and support along the way during my project. You have allowed me to branch out and gain the valuable skills of seeing a project through from the concept testing, prototyping and helping me to develop tests and redesigns to further my work.

Thank you to my girlfriend, Rachel for always being there for me as well especially during these last few weeks as I worked on finalizing the end of my graduate program. Your support means a lot to me and this would have been much more difficult without you in my life.

Thank you to the entire research group for sharing your expertise in various fields with me. It has been greatly appreciated to have such a great pool of knowledge to glean from. Whether it has been helping me with the better programs to make writing much easier or helping me develop models I appreciate it all.

Thank you to my parents for being there for guidance and support during my program and always pushing me to do my best and follow my dreams.

Finally, thank you to the Materials department and program. I have enjoyed how flexible this program was and how I could fine tune both my classes and research to what I feel will help me most on career path.

Table of Contents

Introduction

1.1 Water Scarcity

Water resource management will be the next great problem to solve for the human population. Fresh water access is already a problem in many arid developing countries (Academy, 2017). About 80% of the world's population is exposed to high levels of water security (Mcintyre *et al.*, 2010). This is about 4.8 billion people (based on the study done in 2000) (Mcintyre *et al.*, 2010). Freshwater only makes up ~2.5% of the world's water, two thirds of which, is frozen in the polar ice caps (Sandra, Gretchen and Paul, 1996). The water that humans could use only makes up 0.77% of the available freshwater (Sandra, Gretchen and Paul, 1996). This water is held in bodies of water, aquafers, plants and the atmosphere. Only water that flows through the solar hydrological cycle, such as rain or bodies of water that are in contact with the air, is truly renewable (Sandra, Gretchen and Paul, 1996). Water from aquafers or the ground, can be utilized but then become depleted similar to pumping oil out of the ground (Sandra, Gretchen and Paul, 1996). Water runoff is the main way that humans get water for drinking, industries and agriculture. This typically flows back into rivers, however it is possible to deplete entire rivers of their water supply which can be seen with the Rio Grande (Akasheh, Neale and Jayanthi, 2008). This river no longer reaches the Gulf of Mexico due to high usage from the United States and Mexico (Akasheh, Neale and Jayanthi, 2008). While this is unlikely to be a serious problem in wealthy countries due to their ability to transport freshwater great distances. In developing countries, water will be a limit the growth of developing countries (Academy, 2017). This has led water related health problems and conflicts. These water issues are only predicted to increase as factors such as climate change and population growth increase (Vo and Green, 2000).

1.2 Health problems

More importantly for human use, *clean* water access is a problem especially in developing countries which lack the monetary resources to properly treat water and provide aqueducts to store and transport water among the population. The ability to provide clean drinkable water is the single most important way to improve public health and save lives (Gleick, 2015). This is far from a novel idea, in fact Hippocrates recommended boiling water to kill off the impurities back in 350 BC (Gleick, 2015). In the United States and Europe where water and purification methods are fairly universal greatly decrease the number of hygiene and water borne illnesses in the start of the 20th century (Gleick, 2015). However, in developing countries, where these basic systems are lacking, millions die every year from easily preventable illnesses (Gleick, 2015). Often, the run-off from agricultural pesticides and human and cattle excrement run into rivers (the main water sources) and is then consumed without any purification methods (Gleick, 2015). Nearly 60% of infant mortality in developing countries can be traced back to water sanitation issues (Gleick, 2015). As well as sanitation problems, simply finding access to any water can be extremely burdensome and time intensive. This lack of water may be part of the problem that people aren't practicing proper hygiene habits such as washing hands or purifying water (Gleick, 2015). Time spent looking for water detracts from time being spent in schools as well as greatly limits the ability to grow vegetables which provide essential vitamins to strengthen the immune system (Ashbolt, 2004). Better systems, that are cheap and easier to use, can be utilized to both collect and purify drinking water to help mitigate these preventable deaths. The extreme lack of water also causes more deaths due to struggles over water.

1.3 Water Conflicts History

Conflicts over freshwater are far from a recent argument. Dating back to 2500 BC , in Lagesh, Umma a king rerouted a river away from enemy effectively taking away their water supply and ending the war (Gleick and Heberger, 2013). Throughout history, the importance of having fresh water stores was not overstated. It was a common target during times of war and would cause contention when water supplies were low. More recently, fights over water ownership and access have become more frequent. In the 1880's in New Mexico, there was friction and eventually violence over water rights between ranchers, farmers and villagers (Gleick and Heberger, 2013). In the early 1900's, there were plans to divert the Colorado River to Los Angeles to help it grow, which would take the water away from a small town in California called Owens Valley. The pipeline which was being constructed to do so suffered multiple bombings (Gleick and Heberger, 2013). Eventually however, the water was rerouted to LA and Owens Valley turned into a ghost town due to a lack of water. In the 1970's in China's Zhang River, the villages of Shenxian and Linzhou began fighting over water withdrawals from the river as the river began to dry up from over use. These fights continued for nearly three decades (Gleick and Heberger, 2013). In 1999, Yemen sent a force of 700 troops to stop the fighting in which six people died when two neighboring villages were fighting over a local spring (Gleick and Heberger, 2013). From the early 2000's to now, the amount of disputes over water have increased in the Middle East, China, India and Africa (Gleick and Heberger, 2013). The growing trend being that while water conflicts used to be used more as a military tool, they are now disputes over access to resources. Some of which have resulted in deaths. One way that can help alleviate these problems are by providing other mechanisms to collect water than solely relying on ground and run-off water.

Inspiration and Overview

2.1 Water Collection Methods

There are some methods to collect water from the atmosphere which can help to alleviate the struggle of needing an aquafer or body of water to collect from. Some solutions such as a solar still have been used since the 16th century (Samee *et al.*, 2007). This technique was first used to desalinate water to create both fresh water and salt. It works by covering a body of undrinkable water such as salt or polluted water with a transparent cover such as glass or plastic. As the water heats up, it evaporates and condenses on the covering, which is at an angle, and runs into a collector that is separate from the original body of water (Samee *et al.*, 2007). This is an excellent method to purify dirty water passively, however it does rely on the necessity of having water readily available.

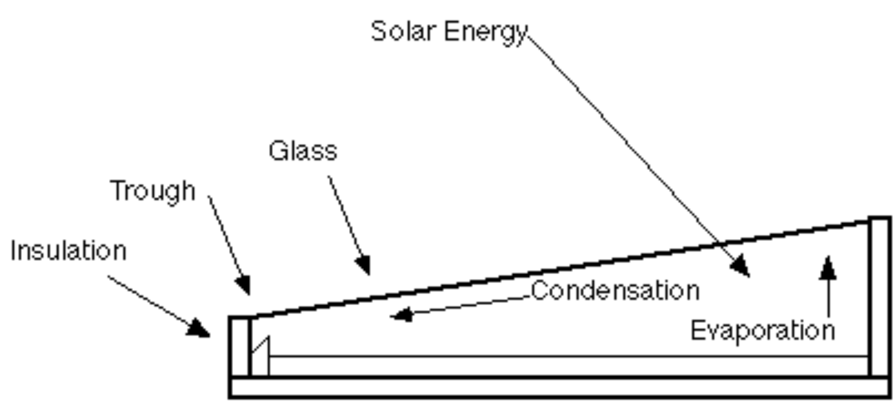

Fig 1. Shows an example of a solar still and how it works by using the sun to evaporate the water out of undrinkable solution and collects it as fresh usable water (Solaqua.com).

Another simple method is to collect the rain water. This is often done by funneling the water run-off from the roof into a collection barrel. There is often a layer of carbon that the water must pass through, which serves as a rudimentary yet effective purification (Fewkes, 2000). This is an extremely affordable and simple system to implement but in areas where precipitation is scarce other systems will be needed to help supplement this water collection method.

An extremely creative way to collect water from fog has been implemented in places such as Chile where fog frequently is blown over desert mountain ranges from the ocean (Academy, 2017). This works by putting up a large piece of mesh that fog passes through. Some of the moisture from the fog condenses on the mesh and once the droplets reach a large enough size they run down the mesh and into a collector, where the water can be used (Gandhidasan and Abualhamayel, 2007). This method is excellent in these types of places where fog is a near daily occurrence. To get enough water for a village multiple 75-100m^2 meshes are used. The one downside to this method, apart from the environmental requirements, is that the fog mesh can be very expensive. They can cost $50 to $150 USD per square meter (Klemm *et al.*, 2012). This is still an excellent method if the environment allows for it. For more methods of water collection, we study the ways in which nature has developed to live in harsh environments.

2.2 Water from Dew

Collecting water from the atmosphere is a great way to obtain a water supply. Atmospheric water is generally clean and be safely used immediately without any extra purification methods. The ancient Greeks were believed to have succeeded in doing this on a large enough scale to supply water to the city of Theodosia (Avenue and Provence, 1996). This is a great alternative source of water for people who live in arid environments. Condensation naturally occurs both in fog and the form of morning dew. Morning dew typically forms a low layer of moisture to the ground of around .3 meters (Avenue and Provence, 1996). This layer can last from one to four hours before the heat of day causes it to evaporate away (Giora J. Kidron, 2000). Depending on the geographic location, the amount of moisture in morning dew may exceed the level precipitation (Giora J. Kidron, 2000). This makes it a viable option for places in the world where the only significant moisture available comes from the low layer of morning dew. In order to determine the best way to help collect and use this low layer of moisture we turned to the natural world to search for examples in order to model our design after.

2.3 Biomimicry

We have seen the problem of fresh water access and the many problems that it is causing all around the world. Often times nature can provide answers to the problems that we as humans face. The natural world is an excellent model of unique solutions to even more unique problems. Life has thrived from the deepest oceans, learned to fly, and fight for precious resources miles above sea level. Plants are surprising resilient to surviving in even the harshest of environments. From windblown trees, high in the alpine to seed pods opening in the heat of a wildfire to be released for germination, plants have found a way not only to exist but to flourish. Manufacturing designs after nature, allows us to model using simple building blocks (Benyus, 1997). This method has been growing in popularity, such as studying leaves to improve solar cells or finding novel biodegradable building blocks. For clues on how to best collect water for human consumption in arid environments, we don’t have to look any further than the cactus.

Often going long durations of time with little or no precipitation it has adapted to being extremely resourceful when it comes to water collection.

2.4 *Gymnocalycium baldianum*

Cactuses are well known for their ability to leave in the desert, where precipitation is sparse and water evaporates quickly. Cactuses typically have very shallow root systems to help even the smallest amount of rain when it penetrates only the upper few centimeters of soil. They can also change their shape slightly to do most their respiration in the evenings when it is cooler to mitigate their water loss during the day (Liu *et al.*, 2015). However, the most unique aspect of a very particular cactus may be the key to creating a novel water collection device that may help humans collect water in arid environments. The *Gymnocalycium baldianum,* native to Argentina, has developed a unique mechanism to collect moisture from morning dew. This brilliant adaptation works by its spines angled in such a way that small droplets of water can form on tips and run down the spines to the base where it is collected by small pores. The spine coupled with tilted scales and splayed capillary tubes along its structure drives water droplets directionally toward the base (Liu *et al.*, 2015).

The spine is at a 15° angle to the cactus and the tilted scales are at a 20° to the spines. Below is a picture of the spine and of a water droplet being forced downward for collection by the cactus.

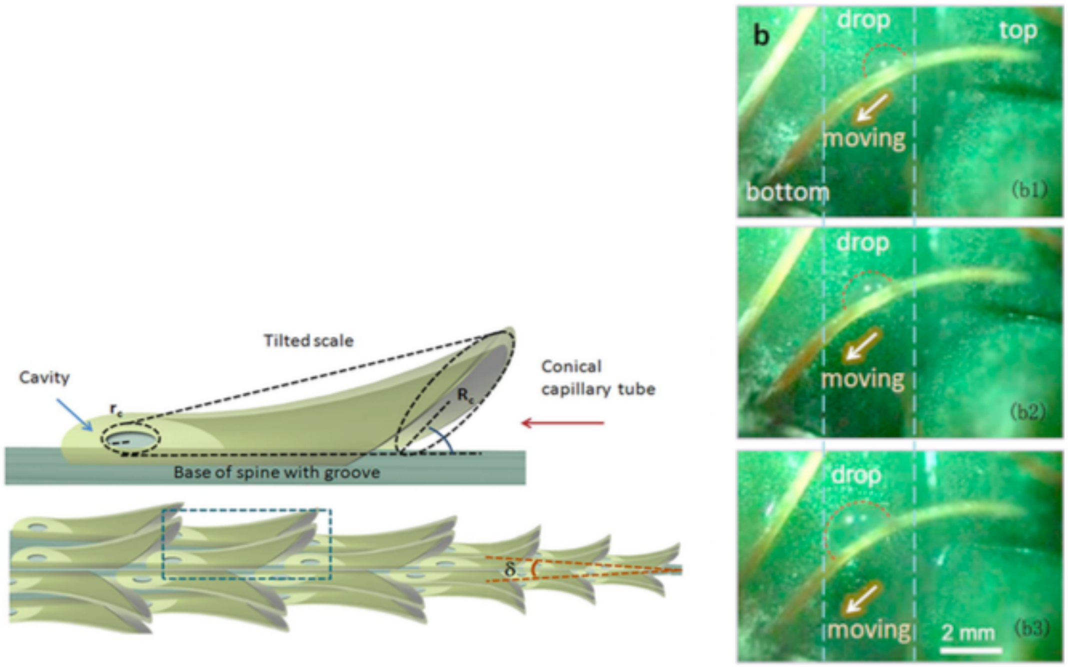

Fig. 2: The picture on the left shows the orientation of the scales in relation to the spine with the capillary tube illustrated as well (Liu *et al.*, 2015). On the right is a photo of a water droplet moving down the spine towards the base (Liu *et al.*, 2015). Both the capillary and a pore at the base of the spine are used to collect the water droplet.

This idea of using a tilted scale to aid in water collection from the available in morning dew was utilized for a novel water collection device from morning dew. To aid in the usability for human use, we began to research possibilities of motion to help capture moisture from morning dew when it is available and store it for later when it is not, such as during the heat of day. The common pine cone is an excellent example of a natural hygromorph, that changes its configuration based on the presence of moisture.

2.5 Pinecone

In order to make this novel device as usable as possible for humans, we wanted a way that it could passively store the collected water during the day. This would allow the users to not need to closely monitor the device every day that there is morning dew and let them collect it on a time frame that works better for them. We studied the pinecone because they open and close their scales based on the absence and presence of water respectively. The pinecone's mechanism of opening and closing was researched to provide answers to our problem.

A pine cone is able to move its scale up to 100°, and works by having two separate layers of scales at the base of the scale (Reyssat and Mahadevan, 2009). One of the layers is an 'active' layer which expands in the presence of moisture and contracts in the absence of it. The other layer is a 'passive' layer, which does not expand or contract with moisture (Reyssat and Mahadevan, 2009). The active layer is on top of the passive layer so when it comes into contact water and expands, it pushes the scale closed. When the active layer dries, it contracts pulling the scale open for seed dispersal (Song *et al.*, 2015). Below is picture of both a pine cone in the open and closed configuration as well as a picture illustrating the angle change of a single scale.

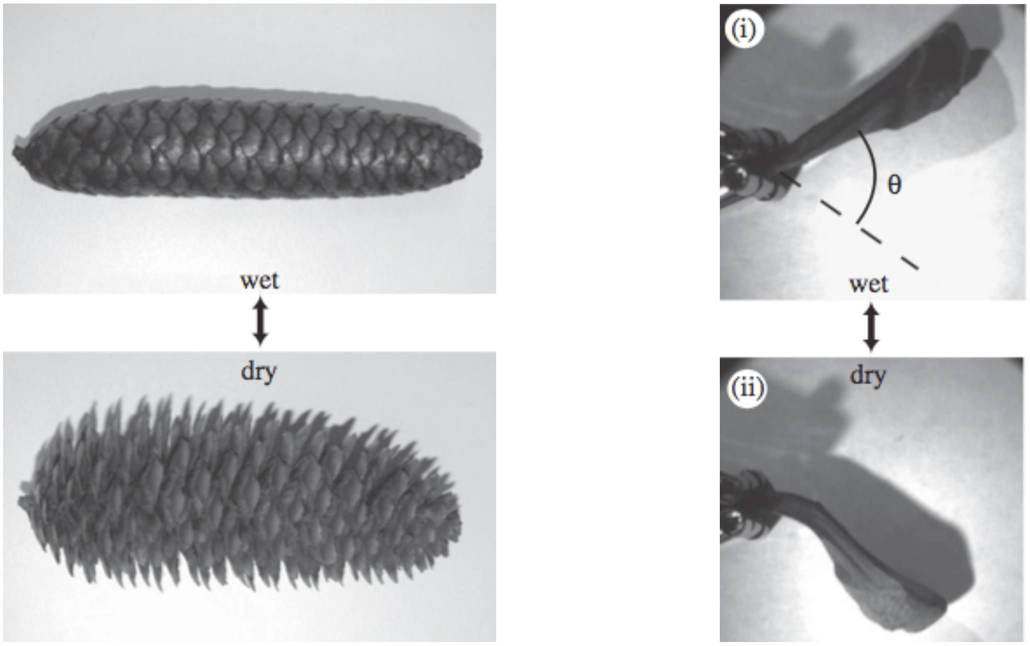

Fig 3. The picture on the left shows a wet and dry pine cone, demonstrating the change in configuration from the presence of moisture (Reyssat and Mahadevan, 2009). On the right, just one scale is showed to illustrate the motion and angle change (Reyssat and Mahadevan, 2009).

The closing of the scale is a capillary driven response so it occurs more quickly than the closing which is based on water's diffusion out of the active layer. This is illustrated by the below graph. The closing of the scale occurs in about 30 minutes but to open takes several hours.

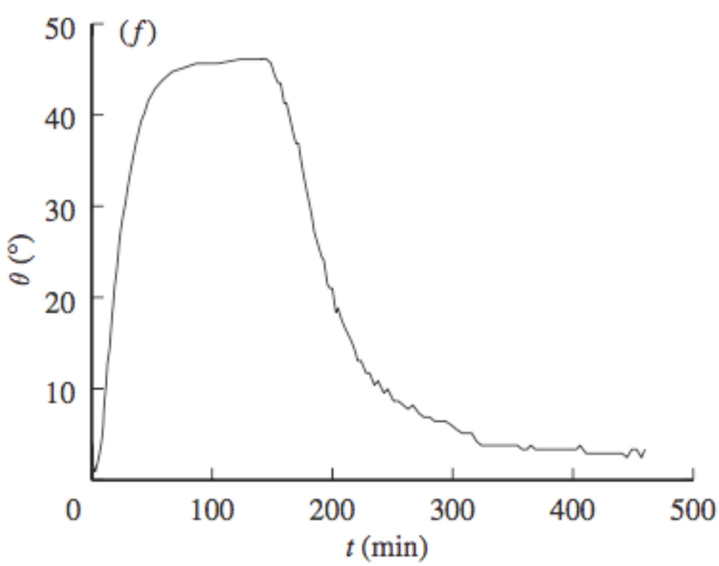

Graph 1. Shows the time of a cycle of open to closed to open (Reyssat and Mahadevan, 2009).

This was used as the basis of opening and closing for our scale system. However, our collection device works in the opposite way by opening in the presence of moisture and closing when it is dry. This will allow our system to passively open during cycles of morning dew to collect the available water and then close during the heat of the day to store the water for later use.

Methods

3.1 Design and Materials

By studying the mechanism of the cactus and the pine we began the development phase of the project. First, we tried a layer of cellulose glued to a polymer like the pinecone. However, we found that while this did create the desired motion there was plastic deformation and would not return fully to its original shape. Then we began to use Poly Lactic Acid (PLA), this allowed for rapid prototypes with 3D printing. PLA was used for fabricating the scales and the collector. The extruder of the 3D printer was heated to 235 degrees Fahrenheit and the bed was heated to 60 degrees Fahrenheit.

To create the desired motion, we used a silica hydrogel that can expand around 40 times its original size. The hydrogel was inserted into a cup on the scale. The cup has many pores along its structure so that the gel is in contact with the outside air. The cup also serves to constrict the expansion of the hydrogel so that only motion in the x-direction will occur. Several scale designs were used to test the effectiveness of different sizes of the silica hydrogel. A rubber band was used to both attach the scales to the collector as well as provide tension for the gel to push against. This also serves as the mode for the scales to return to their original configuration after the gel shrinks in the absence of moisture. The picture below shows the set up that was used for testing.

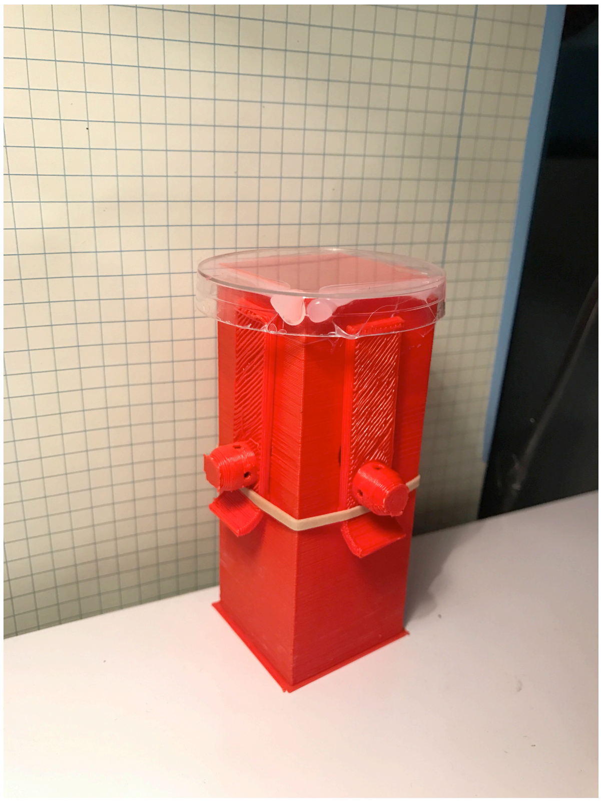

Pic 1. Shows the set up that was used for testing. The red collector and scales were both printed with the PLA. The cup and pores are shown as well as the curved end which allows for a greater ease of angle change. The curved portion of the scale also creates a maximum angle that can occur. A petri dish was used to cover the top of the collect so that any water collected would have to pass through the openings on the collector (which cannot be seen due to the scales).

When the scales are closed as shown above, water cannot enter the collector. As the hydrogel, inside of the scales, swells the scales are pushed open and the water vapor enters the collection device. Below is a series of photos to illustrate how the scales open on the water collection device.

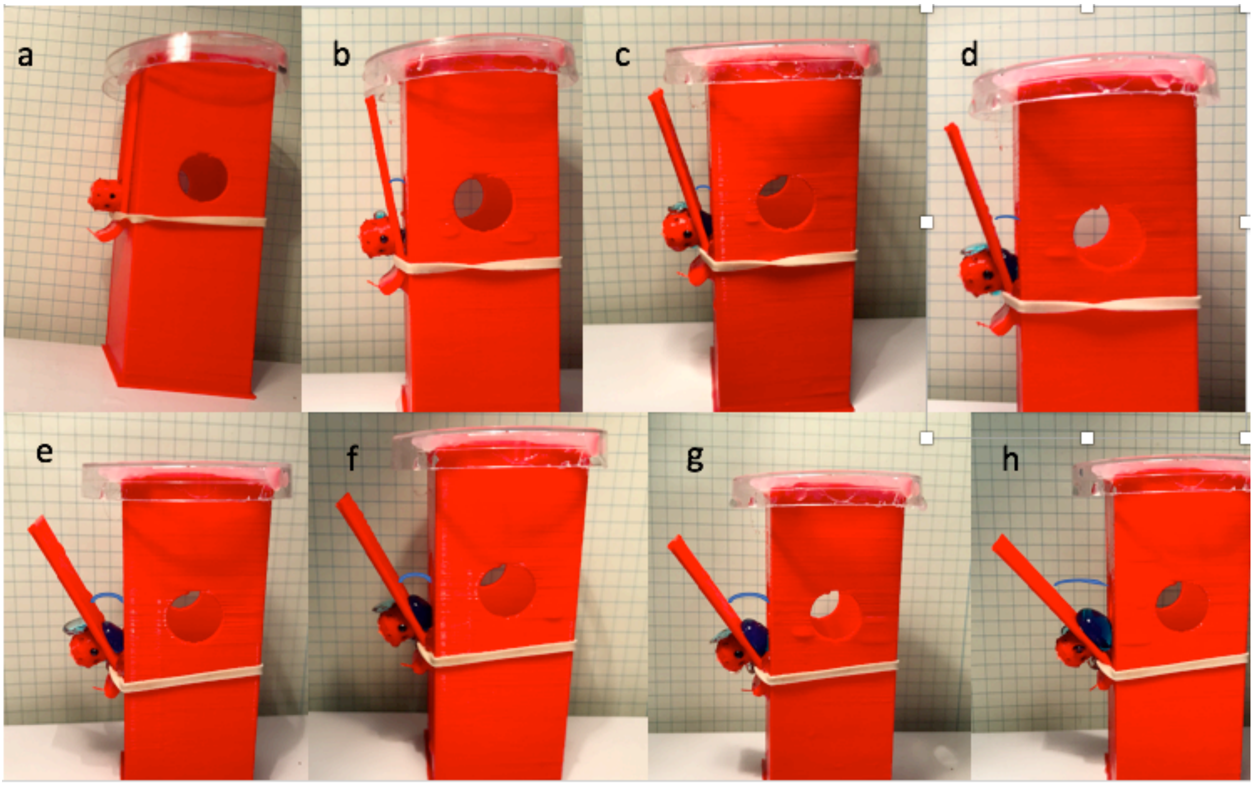

Pic 2. Shows the various stages of the scale opening cycle beginning with a) at time 0 with a 0 degree angle; b) is at 45 minutes with a 10.24 degree angle; c) is at 60 minutes with a 15.46 degree angle; d) is at 75 minutes with 23.57 degree angle; e) is at 90 minutes with a 26.38 degree angle; f) is at 120 minutes with a 32.23 degree angle; g) is at 135 minutes with a 40.12 degree angle and h) is at 150 minutes and has a 45.32 degree angle, at this point the max angle change has occurred. This is a function of the geometry of the curved part of the scale. It serves both as an easier way to initiate the motion as well as limits the angle.

Some of the hydrogel can be seen protruding from one of the pores on the cup of the scale. This serves to help lock the hydrogel in place so that more of its expansion is forced outward in the x direction. The picture shown above is done with hydrogel with a 3 mm diameter. In h), it can be seen that hydrogel expands in all directions once it has exited the cap. This means that the gel doesn't expand only in the x-direction to create motion and some of the expansion is translated to y and z directions creating a slight loss of motion. Below is a more close up picture of this phenomenon.

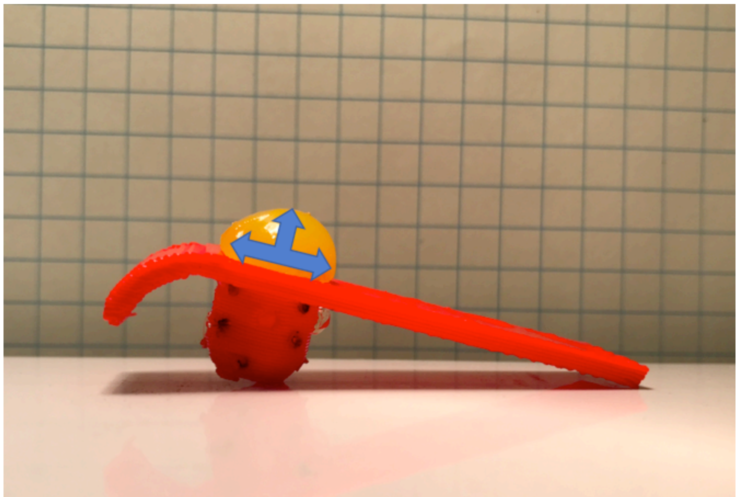

Pic 3. Shows the hydrogel protruding from the cup of the scale. As the gel pushes against the collector the scale is pushed back on the curved section and creates the angle change. Once the gel expands past the opening of the cup, it expands in all directions as illustrated by the blue arrows.

What is promising about this experiment is that the max open angle is reached in less than four hours which is on longer side of a typical duration of a morning dew cycle. This means that during a typical morning dew cycle, which last between 1-4 hours, the scales will be able to open and collect moisture during that time.

As the hydrogel dries, the rubber band pulls the scales closed and stores the captured water. This device was tested to check the effectiveness of various properties of the device. The hydrogel was also measured to create a model in order to compare a theoretical data to empirical data.

3.2 Testing

The opening angle change with respect to time was measured, as well as the closing angle with respect to time. This experiment was repeated with a fully dehydrated hydrogel and a partially hydrated hydrogel to see which would allow for the quickest opening angle change and initiate motion the quickest. The closing angle change with respect to time was measured to determine the water loss due to evaporation that will occur before the scales can close and mitigate this effect. We measured the amount of water collected and calculated the percentage of water that was captured from the available water vapor. The permittivity, chi parameter, cross linking density and shear modulus was also measured from the hydrogel.

3.3 Opening Angle vs. Time

To determine the open angle rate, a humidifier was used to blow water vapor over the scales on the collection device. The experiment was conducted at 20 degrees Celsius. The scales were checked every fifteen minutes to check for any gel deformation. The distance from the tip of the scale to the side of the collector was measured. The dimensions of the scale are 45x15x2 mm in the standard length x width x thickness. The results were recorded in millimeters and then converted to an angle by using the equation below.

$$\theta = sin^{-1}\left(\frac{X}{L}\right) \tag{1}$$

Where x is the distance in millimeters from the tip of the scale from the side of the collector and L is the distance from the bottom of the cap to the tip of scale in millimeters.

This experiment was done with two different sizes of hydrogels in order to get a comparison on how best to maximize the motion of the system. We tested a hydrogel with a diameter of 3 mm and a hydrogel of 9 mm. Each scale had a different size cup to accompany the difference in size of the hydrogel. The cups were designed to provide the tightest fit possible.

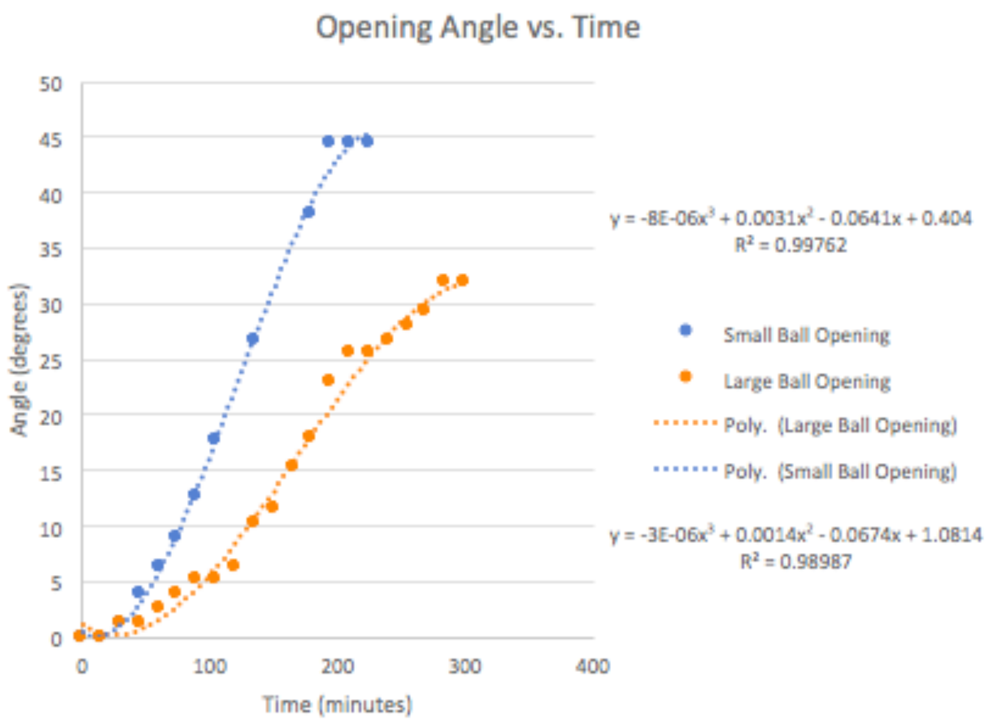

Graph 2. Shows the results from both of the scale opening experiments. Where the angle θ is the y-axis and time in minutes is on the x-axis. The blue line is the smaller hydrogel (3 mm diameter) and the orange line is the larger hydrogel (9 mm diameter). The y=mx+b formula for the small hydrogel and large hydrogel is $y= -8E\text{-}06x^3 + 0.0031x^2 -0.0641x + 0.404$ with a R^2 value of 0.99762 and $y= -3E\text{-}06x^3 + 0.0014x^2 – 0.0674x + 1.0814$ with a R^2 value of 0.98987 respectively.

What can be seen between the two different size hydrogels is that the smaller hydrogel is able to reach the max θ almost 100 minutes more quickly than the larger hydrogel. This is likely because to create the same deflection from the tip the small hydrogel does not have to expand as much as the larger gel. This means a smaller expansion of the gel creates a more drastic angle change. Also the smaller hydrogel is able to reach a greater maximum angle of about 45° compared to the 33° of the larger gel. This is probably because for both scales all dimensions were kept constant and the only change was the cup size to accommodate the varying hydrogel sizes. The smaller gel is able to expand more than the larger gel before the geometric constraints of scale come into effect. Both of these curves are exponential, which is to be expected. Initially, water moisture is only able to contact the gel through the pores in the cup. However, once the gel swells enough to push the scale open, a significantly more about of gel comes into contact with the water vapor and is able to expand more quickly. The tapering off effect at the top of the curve is caused by the curved section of the scale as it stops the expansion from the gel.

The small hydrogel curve is more reminiscent of the opening cycle of a pinecone as shown from graph 1. The opening curve is not as steep as it is for the pine cone. This is likely due to the fact the hydrogel must swell in all directions and is not able apply force solely in the x-direction so some expansion of the gel is not translated to elongation in the x-direction. While the pinecones motion is created by a push-pull mechanism of the difference of the two layers. This may account for a less steep curve as the pinecone. We will create a model as well in the following section that may provide some insight into this phenomenon.

3.4 Closing Angle vs. Time

We wanted to determine how quickly the scales could close. This is important because the quicker they can close the less water will be lost due to evaporation. While the swelling of the hydrogel occurs due to the diffusion rates of water through the gel, the contraction of the hydrogel depends more on evaporation out of the gel. This means that it is likely to be slower than the opening stage of the water collection process. The closing angle with respect to time test was determined by using an oven at 35 degrees Celsius to mimic a high day time temperature. The results were compared by the from the small hydrogel and the large hydrogel to once again see how best to maximize the efficiency of the system.. The angle was calculated by using equation 1, as what was used for the angle opening experiment. The resultant data is shown below.

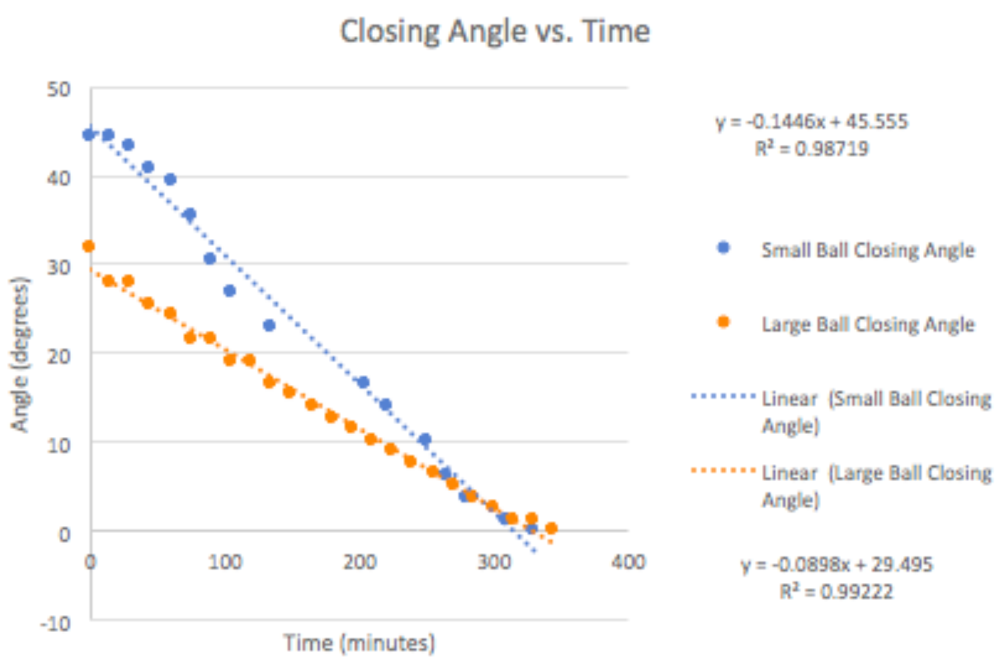

Graph 3. Shows the results from the angle closing test. The blue line is the small hydrogel and the orange line is the large hydrogel. The y=mx+b curve for the small and large hydrogel is y= -0.1446x + 45.555 with a R^2 of 0.98719 and y= -0.0898x + 29.495 with a R^2 of 0.99222

From the data, we found that it while both gels take about the same about of time to close, the smaller gel still closes more quickly. It just a greater distance to travel since it opens ~10° greater than the large gel. Both curves for the gels are linear, perhaps with a slight elongated curve towards the final closing of the last few degrees. Both gels take about 350 minutes to close. This slow closing time since the closing angle depends on the evaporation of water out of the hydrogel, while the opening angle is partially capillary driven as the water is helped through the hydrogel due to the cross-linking. Future work will need to work on better closing mechanisms to help mitigate the water loss while the system is open.

However, this does point to the direction that perhaps different scale geometries can affect the closing rate. Perhaps altering the curve on the back part of the scale so that both gels can only open to the same degrees would affect the closing and likely the opening rate of the smaller gel. This could help to expedite both the opening and closing times of the scales. Both experiments used the same rubber band so they would have equal forces pulling the scales closed.

When we measure the water in the collector before and after the scale closing cycle. We find that the scales do close and store the water but nearly 60% of the water is lost. This experiment is done in an oven that is set at the lowest setting of 35 degrees Celsius. However, the oven temperature cycles between the 35 degrees Celsius and 41 degrees Celsius. The later temperature may be hotter than temperatures that the device would encounter in a real world setting. This may account for the high amount of water loss. Different designs of the scale and collector could help to mitigate the water loss due to evaporation. A lower temperature would help fight evaporation because the gel only depends on the presence of water moisture to close and not the ambient temperatures.

3.5 Water Collection With Scales

The amount of water collected was measured as well. The device was weighed before and after the scale opening experiment and the amount of water in the device was recorded. We also measured the percent of water that was captured compared to the available water. The experiment was done under ideal conditions of 100% humidity at 20 degrees Celsius. The actual amount of water collected during a morning dew cycle may vary from the recorded amounts.

We discovered that the collection device can collect 7 milliliters of water an hour. For the three-hour testing period ~20 mL of water were collected. This experiment was repeated several times and each experiment produced the same result. Since these water collection devices are relatively small. The collectors' dimensions are 5 x 5 x 15cm, with the opening at a height of 12 cm. This means that the total volume available for collection (the volume until the circular openings are reached) is 300 cm^3. 20 cm^3 were collected which is 1/15 of the total available volume. The current dimensions are ideal for water collection of morning dew because a layer of morning dew is usually a low layer of moisture to the ground of about 30cm. Our collection device should be in the middle of that layer if it was directly on the ground.

Multiple systems would be needed to collect enough water for one person for one day. At the current rate of ~20mL for a 3-hour morning dew cycle, 100 devices would be needed to produce 2 liters of water. This means that the devices would be best optimized if placed in a field of some kind. This is good too, because that means that the land could be used for dual purposes such as agriculture. This would further benefit the water collection capabilities because morning dew is partially created by respiration of plants (Avenue and Provence, 1996).

As a comparison, the amount of water collected with the device without the scales attached was measured as well. The experiment was conducted in the same environment as with scales and ran for 3 hours. The device was weighed before and after to calculate the amount of water collected. The total amount of water collected was 18 mL for 3 hours so it collected only 6 mL/hour. Compared to the 7mL that the scaled version collects an hour this is similar. The scales may help funnel the water vapor directly into the collector. This could be in part since the water vapor is entering the container from the top and may then hit the scales and reflect into the collection device. Further re-designs on the scales may help further improve the amount of water collected as well as a hydrophobic coating to aid in the nucleation and transportation of water droplets into the device.

Currently, the way that the device collects water is that once the scales open water vapor flows into the device and condenses on the inside of the collector. This water then flows down and is collected in the bottom of the device. This process could potentially be optimized be a scale design that allows for water that has condensed on the scale to flow down the scale and be deposited into the collector. Since the collector is 3D printed, perhaps a 3D mesh could be printed on the inside of the collector so that there would be more surface area in which water can condense inside of the collector. This would also likely help mitigate the water loss due to evaporation.

Next, the captured water was compared to the total available water. We discovered that currently the device captures 6% of the total available water under ideal conditions. This number is extremely promised because the fog mesh water collection method currently only collects 2% of the available moisture (Klemm *et al.*, 2012). It would be beneficial to test some of the fog mesh under the same conditions as the hygromorphic water collector to get a better side by side comparison.

3.6 Compression Test

We measured the properties of the hydrogel because it is the driving force behind the entire collection device. To measure the cross-linking density, we did a compression test on the hydrogel. Three samples of the gel were fully hydrated ($\phi = .011$), and then cut into cubes. The dimensions of each cube were recorded. The top area was recorded in millimeters as well as the initial height. Each of the cubes were compressed by 10% of its initial height. The amount of weight required to compress the gel was recorded. The following equations were used to calculate the shear modulus (G) and the cross-linking density (ρ_{x}).

$$P_{RR} = \frac{\partial \Psi}{\partial \lambda_R} = 2Gsh\left(\lambda_2 - \frac{1}{\lambda_R^5}\right) \tag{2}$$

Where P_{RR} is the applied pressure which was calculated from the weight/area of the top face. λ is the elongation or the change in height that was measured. The shear modulus was calculated to be 1.10191×10^3.

Then G was used to calculate ρ with the equation below.

$$2G_{sh}\left(\lambda_2 - \frac{1}{\lambda_R^5}\right) = 2\rho_x n k_b T\left(\lambda^2 - \frac{1}{\lambda^5}\right) \tag{3}$$

Where n is the number of moles, k_b is Boltzmann's constant, T is the temperature and λ is still the change in height. $\rho_x = .4234$.

3.7 Free Swelling Test

The gel was also tested to see the change in volume to determine Chi parameter. This experiment was conducted by beginning with a fully dehydrated gel and swelling it. The increase of volume was recorded with respect to time.

$$\rho_x n k_b T\left(\frac{1}{\lambda} - \frac{1}{\lambda^3}\right) - \pi = 0 \tag{4}$$

The term on the left is the elastic force and π represents the osmotic pressure. Osmotic pressure can be found by:

$$\pi = -\frac{k_b T}{v[\ln(1-\phi)+\phi+\chi\phi^2]} \tag{5}$$

Where v is the specific volume of water which is .001 and χ is the Chi parameter. Substituting equation 5 into equation 4 we get:

$$\rho_x n k_b T\left(\frac{1}{\lambda}-\frac{1}{\lambda^3}\right) + -\frac{k_b T}{v[\ln(1-\phi)+\phi+\chi\phi^2]} = 0 \tag{6}$$

And $\phi = \frac{\phi_o}{J} = \frac{\phi_o}{\lambda^3}$ where $\phi_o = 1$ and J is the change in volume. We solve for $\underline{\chi = .3506}$

3.8 Permittivity Test

To determine, the maximum amount of swelling that could occur from the gel in cup, a gel was placed in the cup and fully submerged in water. This provided information about how much water could pass through the pores in the cup and was used to determine how quickly water was able to pass through the cup. The following equations were used to determine cup's permeability.

$$r(t) = rf\,[1-\exp^{-\alpha t}] \tag{7}$$

And

$$\alpha = \frac{\kappa}{R^2} \tag{8}$$

Where κ is the amount of elongation of the hydrogel. Using a best fit curve to the data, we found rf to be .55 and α to be .00027. The graph below shows this equation fit over the experimental data.

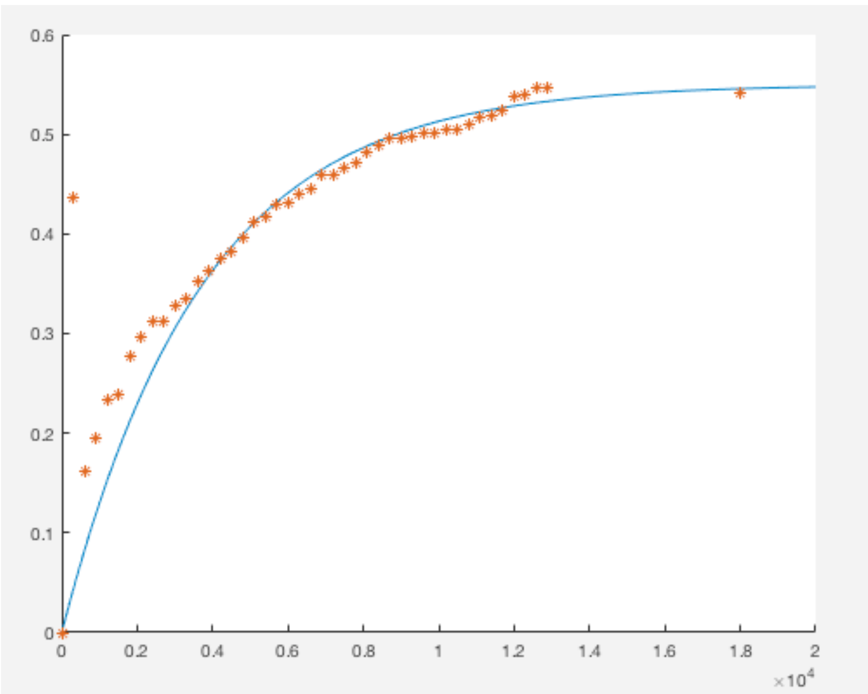

Graph 4. Shows the best fit line juxtaposed on top of the experimental data to solve for rf and α.

The data acquired from the compression, free swelling and permittivity tests were utilized in the creation of a model of how hydrogel will react in regards to the angle change. This model was compared to the empirical data that was calculated and illustrated above to help and create the most effective version of our water collection device.

Hydrogel Model

4.1 Assumptions

To create a model of the hydrogel to optimize our performance we had to make some assumptions and parameters to put into the MATLAB program. The first assumption we made is that we will begin with a fully dehydrated hydrogel, $\phi = 1$. This serves to model the most realistic performance of the gel because if it were subjected to a natural environment, the gel would completely dehydrate if there is no or low moisture present.

We assume that initially, during a hydration cycle, that water only enters the gel through the pores in the cap and not through the main opening. This explains the initial exponential curve that we see from our experimental data. Initially the gel swells in all directions until it reaches the constraints of the cap. At that point the gel is forced outward, after the gel has reached a specific volume fraction. Here we assume that water is only entering the gel from the exposed opening. We assume that the water entering from the pores is insignificant compared to the water entering the exposed gel. The images below illustrate this effect.

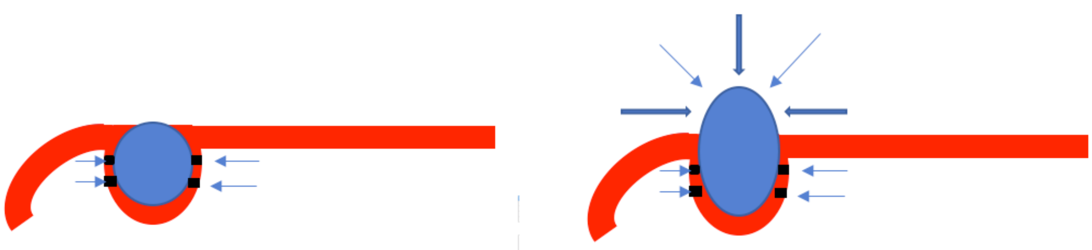

Fig 4. Shows the initial and final states of water entering a cross section of the hydrogel. On the left, the initial condition is shown, water cannot enter through the main opening because it is pressed against the water collector, so water may only enter through the pores (black) which is illustrated by the blue arrows. On the right, the hydrogel has expanded out of the cup and is now exposed to the available water moisture. The exposed surface area if significantly more than just the pores.

All of the parameters such as G, χ, cross linking density, α and rf were calculated from the tests in the previous sections. The boundary conditions used for the model were that there is zero flux in the center of the hydrogel and that ϕ=1 at the surface in contact with the collector. They were incorporated into the model as well. This model assumes that water only enters from the main opening in the cup and that *all* the motion will be translated into the x-direction. The shape assumed to be a cylinder because a half dome would not allow for a boundary condition and if we used a sphere, there would be backwards force which makes the curve of the model not as steep as what we measured empirically. Next we needed to determine a formula that we could use to model our hydrogel. We used a modified version of Fourier's Law to accomplish this goal.

4.2 Fick's Law

To optimize the performance of this water collection device, we wanted to see what the theoretical capabilities of our hydrogel were. A model was created based from equation for heat expansion. We decided that this hydrogel will behave very similarly to this formula except for the temperature variable which creates the expansion of the material will be replaced by the volume fraction of the hydrogel for our use. We will solve Fick's Law of one dimension and then modify the final solution to fit our needs. We begin with the derivation of Fick's Law for one dimension since we only care about the expansion in the x-direction since that will create the motion of our scales.

We calculated α by fitting a curve to our experimental data as shown in Graph 5. Which was done with the following equation.

$$r(t) = rf\,[1-\exp^{-\alpha t}] \qquad (9)s$$

We change the boundary conditions to modify this formula for use of our hydrogel. We also take u to replace temperature with the volume fraction of the hydrogel. We also assumed that our hydrogel would behave like a cylinder do the confines of its cup and that a cylinder would provide the greatest motion in the x-direction. Other shape configurations were considered but ultimately thrown out due to lack of boundary conditions or inaccuracies. The other shapes will be discussed in the following section.

Our initial conditions is that $\phi(L,t) = 1$ because initially the hydrogel begins with a volume fraction of 1. The other boundary condition is that $f(x)=1$ everywhere. Using these boundary conditions and solution of a 1D Fick's Law we solved for above we solve for the heat equation using a Fourier series. We begin with equation 19, where we have ϕ as a function of space and time $\phi=\phi\ (x,t)$. Recall that for our purpose, the variable u represents the volume fraction. We set our boundary conditions that at $\frac{\partial\phi}{\partial x}=0$, $\phi(L,t)=1$because that is the fully dehydrated hydrogel. Our other initial condition is that $f(x)=1$ everywhere. With these two boundary conditions, we proceed to the initial steps of the solution.

$$\frac{\partial\emptyset}{\partial t}-\alpha\left(\frac{\partial^2\emptyset}{\partial x^2}\right)=0 \tag{10}$$

We solve equation 10 to get our solution shown below. The full derivation is in A1. of the appendix. We plot our model and summated to n=20.

$$\phi(x,t)=\sum_{n=1}^{20}\mathrm{DnCos}\left(\frac{2n+1}{2L}\pi x\right)\ e\left(\frac{-n^2\pi^2\alpha}{L^2}t\right) \tag{29}$$

And

$$\mathrm{Dn} = \frac{2}{\mathrm{L}}\int_0^L \mathrm{Cos}\left(\frac{2\mathrm{n}+1}{2\mathrm{L}}\pi\mathrm{x}\right)\,\mathrm{dx} \tag{30}$$

This is the general solution for the heat equation slightly modified for our purposes. However, because the volume fraction only depends on time and space we need to find a way to remove x component from equation (29). In order to do this, we take the average x value by integrating the solution from 0 to L_0. This removes the x value giving the following.

$$\bar{\phi}(\mathrm{t}) = \frac{1}{L_o}\int_0^{L_o} \phi(\mathrm{x}) = \sum_{n=1}^{20}\left(\frac{n}{2}\right) D_n\text{-}\left(\frac{2}{2n}+1\right)\pi\sin\left(2n+\frac{1}{2L}\pi\right)e^{\left(-\frac{\pi^2 n^2 \alpha}{L}t\right)} \tag{31}$$

Where the volume fraction is given as a function of time. L is the hydrogel's final diameter and n is an integer from 1 to 20, t is time which we input 300 seconds so we could better relate the model to the experimental data which was done on 900 second intervals. However, 900 seconds in the model did give a very good curve because the points were too far apart. Next we converted the volume fraction to elongation by the following formula.

$$\lambda(\mathrm{t}) = \frac{1}{\bar{\phi}(\mathrm{t})} \tag{32}$$

By using the relationship between elongation and the change in length we solve for the final length of the hydrogel by the equation below

$$L(t) = L_o\bar{\lambda}(\mathrm{t}) \tag{33}$$

L(t) was input into a modified version of equation (1) which states $\theta = sin^{-1}\left(\frac{x}{l}\right)$, to convert it to degrees. To find the angle from the hydrogel expansion we used, $\theta = sin^{-1}\left(\frac{L(t)}{l}\right)$. Where L(t) is the final length and 'l' is the distance from the end of the scale to the hydrogel as shown in the model. Then it is divided by small l which is the distance from the bottom of the cap to the midpoint of the gel that comes into contact with the collection device. The inverse sin of this answer is taken to convert the data into degrees. This data was plotted next to the experimental data so that we could better compare the information from the model. The diagram below illustrates how the angle was calculated.

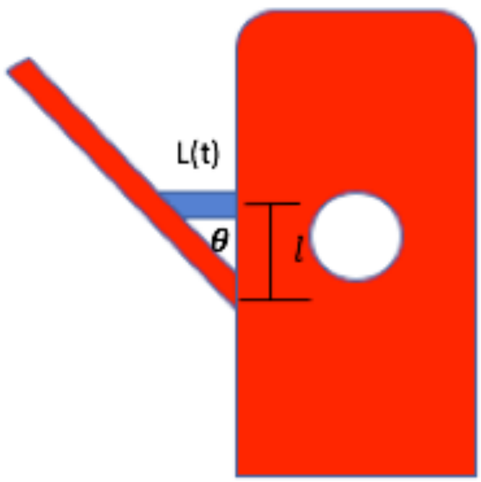

Figure 5. Illustrates how the model data was converted to degrees, where x is the distance of the hydrogel protruding from the scale (shown in blue) which was calculated by the formula above. The distance the bottom of the cap (not shown) to the midpoint that the hydrogel contacts the collector is denoted by 'l'. This was used to create the angle from equation (1)

The resultant data was compared to our experimental data to provide clues for improvement. The solution shows the effects on volume fraction with respect to time. We ran the model for various sizes of gels to find how to help theoretically determine. To change this, we input several different diameters as well as the ones that we experimentally recorded to test the accuracy of our model. We also changed the permeability of the gel to see test if perhaps using a gel with a greater permeability would allow for a greater expansion rate.

4.4 Model Data and Comparison

After we put the formula into MATLAB and solved the equation, it created a graph that looked fairly similar to our experimental data. The graph of the model is below.

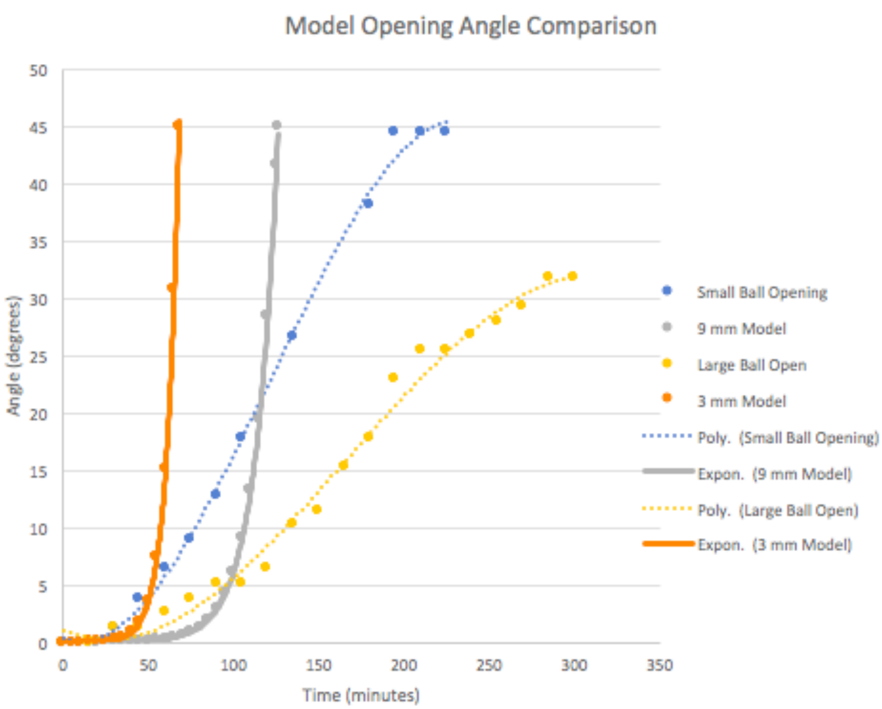

Graph 5. Shows the model data for two different size hydrogels compared to the experimental data. On the furthest left (orange solid line) shows the model data for a 3 mm hydrogel and the gray solid line shows the prediction for a 9 mm hydrogel

The orange and gray solid lines on the left are the model obtained from the previous equations. It is a good approximation of what we were able to measure with our system. The model data was converted to degrees in order to view it side by side with the experimental data. The model data, in degrees, was plotted next to the experimental data.

Viewing the graphs side by side with the experimental data shows that the model is a decent approximation in terms of the time that it takes to initiate motion and that we made the correct assumptions in its design. However, there are some differences between the experimental and theoretical data. The model does correlate with the experimental data that the smaller the gel the faster the opening motion occurs. However, both of the modeled curves have the same slope but differ in the amount of time that it takes for motion to occur.

The model solely demonstrates exponential growth because it does not take into effect the elasticity of the hydrogel. For both hydrogel sizes, It assumes that water will continue to enter the gel until an equilibrium is met. It is a steeper curve because it assumes that all of the expansion will be in the positive x direction. The model also assumes that all the water will enter the hydrogel through the main opening and not through the pores. We decided that while this is not the actual way that our device works, this is a very good approximation because once the gel is exposed through the main opening, the water entering through the pores on the periphery of the cup will be insignificant to the amount entering the exposed hydrogel.

What is promising is that for both the model and the experimental data, is that for the smaller gel, they both take about 45 minutes to begin moving while for the larger hydrogel, the model takes about 90 minutes. This is due to the fact that it assumes all of the water is entering through the main opening and not through the pores. This may account for the difference of the opening time. Also, the model assumes that all of the elongation is happening in the positive x-direction. In actuality the gel expands in all directions and once it fills the confines of its cup, the gel is forced to swell outward. We know that this is the case from our measurements of the hydrogels with different diameters. The gel with the larger diameter, has a much shallower slope than the experiment with the gel with a smaller diameter.

Another difference between the model and the experimental data that could help to explain the difference in slopes is that the model neglects to include the resistance of both the rubber band and the collector pushing back on the gel as it expands. An ideal system would provide little to no resistance while the gel is expanding and increase the resistance during a closing cycle. Perhaps this could provide clues to a better mechanism to help the scales open and close.

The last difference between the model and empirical data is that may explain the difference of the slopes is that, while the model assumes a cylinder which translate all its elongation into forward motion, the gel swells outward in a dome. This means that some of the expansion of the gel is lost in the y and z directions. This model assumed only a one dimension. However, if we assumed the gel swelled in a dome shape we would not have been able to calculate an analytical solution because there would not have been any boundary conditions in which to base our formula. We will explore other possibilities to make improvements or substitutions in our water collection device in the following section. The model points to the conclusion that as we decrease the size of the gel, the opening time will also decrease. To determine other possibilities of improvement we also modeled the changing the permeability of the gel.

4.5 Permeability and Opening Time

The permeability (α) used in the first model data was found experimentally from Graph 4. We tested the possibility of increasing the permeability. This would represent using a different hydrogel with different properties. We modeled several possibilities to determine what could be ideal properties to be used as a hydrogel for future work. The resultant data is show below compared to just the smaller hydrogel for ease of discerning the differences. We changed α by a factor of $\pm$ 10 to see the effects that permeability can have on the opening rate.

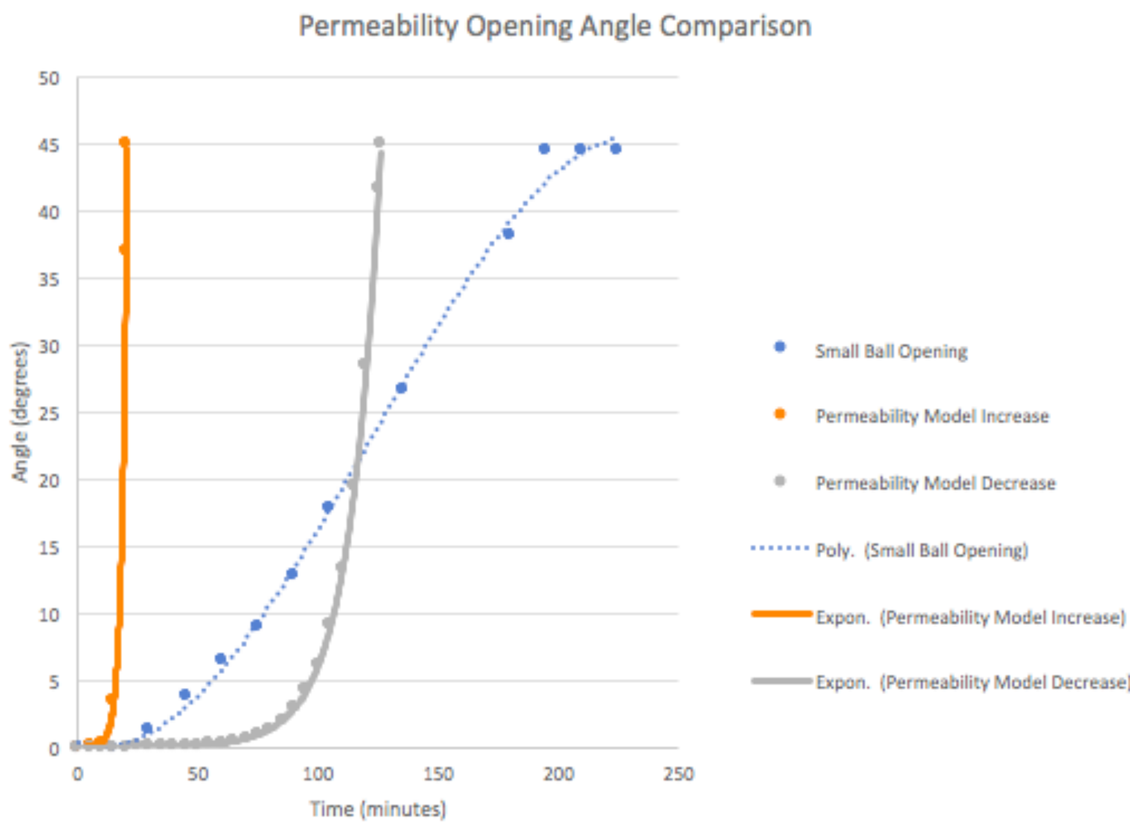

Graph 6**.** Shows the effects of permeability on the system. The orange line represents increasing the permeability while the gray line represents decreasing the permeability. The model data is compared to the opening angle experimental data done with the 3 mm hydrogel.

By examining this model data it is clear that, by increasing the permeability water will be able to enter the hydrogel more quickly and thus the gel will more rapidly expand and push the scale open. By decreasing the permeability water takes longer to enter the gel and the opening mechanism happens more slowly. This provides promising data because it suggests that if the scale opens more quickly because water can enter gel more easily that it may also close more rapidly because the water would have an easier time exiting the system. Future work will examine the possibility of using a more permeable gel to expedite both the opening and closing procedures.

The model also could provide information about how the system operates under differing amounts of humidity. However, our experimental set can only do 100% humidity from blowing water vapor directly at the scale. The ambient air's humidity ranges from 16%-20% in the lab and slightly less in the oven. The gel was tested in an environmental chamber; however, the chamber could only reach a maximum humidity of 40%, which was not enough to change the size of the gel. It is likely that the gel only truly functions in 100% humidity, which is beneficial because anytime morning dew is present the humidity will be 100%. If the scales opened in less than 100% humidity, it could affect the closing rates and the ability of the scales to stay closed during the heat of the day if it is humid outside. It is possible that if a different gel is used with a greater permeability that it may absorb some degree of water in environments with a high degree of humidity. This is something that would have to be investigated as well. The model provided valuable information about the current process of the device and ways that it could be improved for better usability in the future.

Conclusions and Future Work

5.1 Summary

“Water water everywhere nor any drop to drink” –Samual Taylor Coleride. While this poem was about a sailor who ran out of fresh water while at sea. It is also relevant to many parts of the world that do not have access to fresh water or the water they do have access to is polluted. Water shortages are already a problem and as the global population continues to grow access to fresh water may be a luxury only the wealthy can afford. As climate change increases, as well, leading to more and more droughts in parts of the world the problems we are seeing will be amplified.

Already millions of people are dying from health-related issues to water. This is in part from water borne illnesses from drinking contaminated water as well as water scarcity. Water scarcity leads to people skipping basic hygiene such as washing hands and bathing because there isn’t enough water around to drink and clean oneself. This is a major problem in developing countries where the water that flows back into rivers contains fecal matter and pesticides from agriculture. In places where there isn’t ground water, people are having to travel many hours to obtain water. This takes time away from going to school, house hold chores and jobs. Often in developing countries it is the women and children who go on this missions every day. This is part of the reason, that women are not joining the work force and gaining more independence, because they simply do not have the time to do so.

In addition to sicknesses, and lack of hygiene from water shortages there is also a growing amount of violent conflicts occurring in the world. Historically, fresh water stocks were attacked as a military maneuver to stop an enemy in their tracks. Today we are seeing many villages having violent confrontation over water rights and access. It is predicted that these conflicts will increase as global warming causes more droughts in parts of the world. It is vital to start now to solve these problems before they escalate.

There are many organizations working with developing countries to help install water collection methods to alleviate the many water related problems that exist. One of the most common ways to collect water is simply rain water catchment systems. To do this, houses are outfitted with gutters that funnel water from rain into a barrel for storage. The water passes through a layer of carbon, which acts to filter out impurities so that water doesn't go bad. This is often done by education about how to install these systems in various parts of the world.

Other mechanisms of water collection are the solar still, which is an old way of collecting water, this works by using solar energy to evaporate fresh water out of undrinkable sources and collecting the water that condenses on the covering of the solar still. This is a simply method of water collection but is only practical if there are existing stores of undrinkable water. This limits the spatial distribution of this method.

Another innovative way to collect water is by using large pieces of mesh to collect water from fog. This is an excellent way of collect water in places where precipitation is low but heavy fog is prevalent, such as Chile, where fog blows in from the ocean. As the fog passes through the mesh, some of the water condenses on the mesh where it then runs down and is collected. Large pieces of mesh of around 75-100m^2 are used to accomplish this goal. The fog mesh can collect 2% of the available water as fog passes through it and is dependent on the amount of surface area in the mesh.

There are places in the world where, such as Tanzania and Israel where the level of annual precipitation is surpassed by the amount of morning dew. This leaves a niche for a novel device that can collect water from morning dew and store it so that it may be used for human consumption. This is a good collection method because atmospheric water is generally pretty clean and can consumed immediately without any further purification treatment. By studying the way in which a cactus can collect water from morning dew and the movement of the scales of a pinecone we developing a collection device with hygromorphic scales that open in the presence of water to collect the vapor from morning dew and will then close to store it in the heat of the day.

The initial data is promising but still has room to be optimized. We found by changing the volume fraction of the hydrogel used we could increase the time that it took for the scales to open by almost 100 minutes. The scales also can open within 40 minutes which is good because the typical morning dew cycle lasts for about one to four hours. We found that under ideal conditions of 100% humidity, our device can collect 7mL/hour. It also collected 6% of the available moisture. If many of these devices were placed in a field, they may provide enough water for a village to use. The benefit of using a field for the device's installation is that morning dew is produced by the respiration of plants and that the field can still be used for other purposes such as agriculture.

5.2 Future Work

While our data is auspicious, there is still room for improvement. The scale design can be altered to allow water to condense on the scale and drip directly into the collector. If the device was made slightly large it could accommodate more scales which could also increase its efficiency. If the water collector had a 3D mesh on the inside it would increase the surface area for water to condense around as it passes through the openings on the side. This may also help combat evaporation because it makes a more difficult path for water vapor to leave the device while the scales are closing in the heat of the day. Perhaps the shape of the hydrogel could be modified into a cylinder so that more of its expansion is translated to pushing the scales open. Different curvature of the scale could be tested to see if the closing time of the scale could be increased, or perhaps a stronger spring tension to aid the scale in closing. The faster, we can get the scale to close the less water we will lose to evaporation. Currently about 60% of the water is lost to evaporation. If multiple of the devices are connected by piping, the water from all the devices could be collected at once. This could help fight evaporation while the scales close as well. If the areas where this is implemented already have access to drinking water, this may be used as an irrigation system for agriculture which can help to provide better nutrition for impoverished parts of the world.

From our model data, we find that different hydrogels with greater permeability could be used to increase the opening and closing rates of the scales, this would help both in the collection of water and the storage of it. Perhaps the scale geometry could be modified to optimize the angle, which could also help the opening process, for example the smaller hydrogel wouldn't have to open to such a large angle.

5.3 Implications

The implications of the data we have collected show that this device is a viable mechanism for water collection and storage. It could help alleviate the problems of water shortages in areas in the world where water from morning dew surpasses annual precipitation. While it may not solve 100% of the water shortages, its low cost to create and passive collection mechanism make it an attractive option for atmospheric water collection. If multiple of these devices were used in the right conditions it could provide drinking water for a village, or help to irrigate a field. The information and data points that this system could work and a time may come where innovative devices like this are need to help the world with the growing problem of water shortages.

References

Academy, R. S. (2017) 'Fog-water Collection in Arid Coasta Locations', 20(7), pp. 303–308.

Akasheh, O. Z. Ã., Neale, C. M. U. and Jayanthi, H. (2008) 'Detailed mapping of riparian vegetation in the middle Rio Grande River using high resolution multi-spectral airborne remote sensing', 72, pp. 1734–1744. doi: 10.1016/j.jaridenv.2008.03.014.

Ashbolt, N. J. (2004) 'Microbial contamination of drinking water and disease outcomes in developing regions', 198, pp. 229–238. doi: 10.1016/j.tox.2004.01.030.

Avenue, L. and Provence, U. De (1996) 'Water recovery from dew', 182, pp. 19–35.

Benyus, J. M. (1997) 'Biomimicry: Innovation Inspired By Nature'.

Fewkes, A. (2000) 'Modelling the performance of rainwater collection systems : towards a generalised approach', 1(1999), pp. 323–333.

Gandhidasan, P. and Abualhamayel, H. I. (2007) 'Fog collection as a source of fresh water supply in the Kingdom of Saudi Arabia', 21, pp. 19–25. doi: 10.1111/j.1747-6593.2006.00041.x.

Giora J. Kidron, A. Y. and A. (2000) 'Dew variability within a small arid drainage basin in the Negev Highlands ', *The Hebrew University*, pp. 63–80.

Gleick, P. H. (2015) 'Dirty Water : Estimated Deaths from Water-Related Diseases 2000-2020', pp. 1–12.

Gleick, P. H. and Heberger, M. (2013) 'Water Conflict Chronology', pp. 173–219.

Klemm, O., Schemenauer, R. S., Lummerich, A., Cereceda, P., Marzol, V., Corell, D., Heerden, J. Van, Reinhard,

D., Gherezghiher, T., Olivier, J., Osses, P., Sarsour, J. and Frost, E. (2012) 'Fog as a Fresh-Water Resource : Overview and Perspectives', 1998, pp. 221–234. doi: 10.1007/s13280-012-0247-8.

Liu, C., Xue, Y., Chen, Y. and Zheng, Y. (2015) 'Effective directional self-gathering of drops on spine of cactus with splayed capillary arrays', *Scientific Reports*. doi: 10.1038/srep17757.

Mcintyre, P. B., Gessner, M. O., Dudgeon, D., Prusevich, A., Green, P., Glidden, S., Bunn, S. E., Vo, C. J., Sullivan, C. A., Liermann, C. R. and Davies, P. M. (2010) 'Global threats to human water security and river biodiversity'. doi: 10.1038/nature09440.

Reyssat, E. and Mahadevan, L. (2009) 'Hygromorphs: from pine cones to biomimetic bilayers', *Journal of Royal Society Interface*, (6), pp. 951–957. doi: 10.1098/rsif.2009.0184.

Samee, M. A., Ã, U. K. M., Majeed, T. and Ahmad, N. (2007) 'Design and performance of a simple single basin solar still', 11, pp. 543–549. doi: 10.1016/j.rser.2005.03.003.

Sandra, L., Gretchen, C. and Paul, R. (1996) 'Human appropriation of renewable fresh water'.

Song, K., Yeom, E., Seo, S.-J., Kim, K., Kim, H., Lim, J.-H. and Lee, S. J. (2015) 'Journey of water in pine cones', *Scientific Reports*. doi: 10.1038/srep09963.

Vo, C. J. and Green, P. (2000) 'Global Water Resources : Vulnerability from Climate Change and Population Growth', 289(JULY).

Appendix

A.1 Derivation

$$\mathbf{q} = -k\nabla u \tag{11}$$

Where k is the thermal conductivity and u is the temperature across a gradient. Since we are only solving for q in one dimension we can use the following equation. If we were solving for three dimensions we would also have to take the derivative of u with respect to y and z as well.

$$q = -k\frac{\partial u}{\partial x} \tag{12}$$

Next we need to solve for the internal energy per unit volume.

$$\Delta Q = c_p \rho \Delta u \qquad (13)$$

Where ΔQ is the internal energy per unit volume, c_p is the specific heat capacity and ρ is the density. We can divide this equation through by ρ so that the volume will change to mass and the masses cancel out. We then get the following equation:

$$Q = c_p \rho u \qquad (14)$$

Then we must define our length. If we take a cylinder and take a cross section of it we can define are length as the distance between $x\text{-}\Delta x \le \varepsilon \le x+\Delta x$ over the time period; $t\text{-}\Delta t \le \tau \le t+\Delta t$. We can now integrate over the cross section.

$$c_p \rho \int_{x-\Delta x}^{x+\Delta x} [u(\varepsilon, t+\Delta t) - u(\varepsilon, t\text{-}\Delta t)] d\varepsilon = c_p \rho \int_{t\text{-}\Delta t}^{t\text{-}\Delta t} \int_{x-\Delta x}^{x+\Delta x} \frac{\partial u}{\partial \tau} d\varepsilon \partial \tau \qquad (15)$$

Where ε is some position at a later time minus ε at an earlier time. Then using the definition of a derivative, we can create the right side of equation (13). If work = 0 and there is no gradient, ΔQ can be determined entirely by the solvent flux. However, for our purposes, ΔQ would be accounted for by the flux of water across the cross section. Fick's law dictates equation (14) below where once again the definition of a derivative is used.

$$k \int_{t-\Delta t}^{t+\Delta t} \left[\frac{\partial u}{\partial x(x+\Delta x, \tau)} - \frac{\partial u}{\partial x(x-\Delta x, \tau)} \right] d\tau = k \int_{t\text{-}\Delta t}^{t\text{-}\Delta xt} \int_{x-\Delta x}^{x+\Delta x} \frac{\partial^2 u}{\partial^2 \varepsilon} d\varepsilon \, d\tau \qquad (16)$$

By the conservation of energy, we know that the equation below must equal zero.

$$\int_{t-\Delta t}^{t+\Delta t}\int_{x\text{-}\Delta x}^{x+\Delta x}[c_p\rho u_\tau\text{-}ku_{\varepsilon\varepsilon}]\, d\varepsilon\, d\tau \;=\; 0 \tag{17}$$

Since this is true, we know that what is inside the brackets must equal zero because of conservation of energy.

$$c_p\rho u_t\text{-}ku_{xx} = 0 \tag{18}$$

We rearrange this equation to solve for u_t.

$$u_t = \frac{k}{c_p\rho}u_{xx} \tag{19}$$

Conveniently we can substitute in α to get rid of k, $c_{p,}$ and ρ by the following equation. This is ideal because we don't have to find an equivalent of the specific heat capacity and thermal conductivity that would apply to our expanding hydrogel.

$$\alpha= \frac{k}{c_p\rho} \tag{20}$$

Substituting this into equation (17) we get our solution for one dimension.

$$u_t=\alpha u_{xx} \tag{21}$$

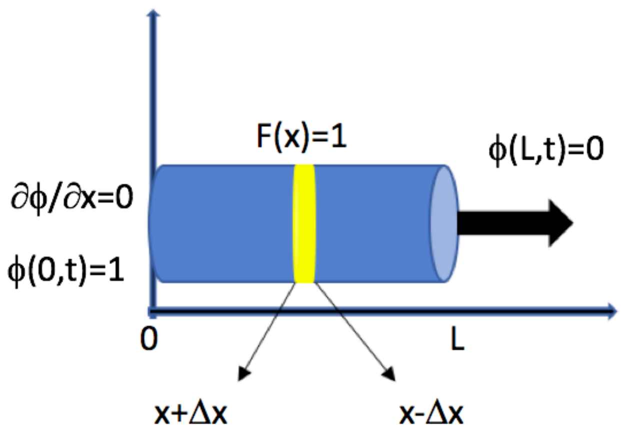

Fig 6. Shows the boundary conditions of the problem as well as the assumptions made to solve Fourier's Law in the previous section.

$$\phi(x,t) = X(x)T(t) \tag{22}$$

By using the separation of variables we create the following equation. Here we will substitute ϕ in for the place of temperature.

$$\phi' \frac{t}{\alpha\phi(t)} = \frac{X''(x)}{X(x)} \tag{23}$$

Because the right side of the equation only depends on x, the spatial variable, and the right side only depends on time. Both sides are equal to some constant value $-\lambda$. We can then create following equations.

$$\phi' \frac{t}{\alpha\phi(t)} = -\lambda, \phi'(t) = -\lambda\alpha\phi(t) \tag{24}$$

And

$$\frac{X''(x)}{X(x)} = -\lambda, X''(x) = -\lambda X(x) \quad (25)$$

We know that $\lambda \leq 0$ cannot exist, to prove this we suppose that λ is less than zero and solve for our volume fraction. We use real number B and C.

$$X(x) = Be^{\sqrt{-\lambda x}} + Ce^{-\sqrt{-\lambda x}} \quad (26)$$

From our boundary conditions, we get X(0) = 0 = L, is this is true than B and C must also equal zero. This implies that our volume fraction is zero which violates our boundary condition. If we suppose that λ=0 and solve for that. We again will use real numbers B and C.

Thus X(x) = Bx + C, we also find that ϕ=0. Therefore we ascertain that λ must be greater than zero. Using this, we obtain the following formulas using real numbers A,B and C.

$$\phi(t)=Ae^{-\lambda\alpha t} \quad (27)$$

$$X(x) = B\sin(\sqrt{\lambda}x) + C\cos(\sqrt{\lambda}x) \quad (28)$$

And

$$\sqrt{\lambda} = n\frac{\pi}{2L} \quad (29)$$

From our initial boundary condition, we conclude that for $\partial\phi/\partial x=0$ to be true B=0 and since our hydrogel is elongating from 0 to L, that $\sqrt{\lambda}$ must equal $n*\pi/2L$. We then solve for the general solution below

$$\phi(x,t) = \sum_{n=1}^{\infty} \mathrm{DnCos}\left(2n + \frac{1}{2L\pi x}\right) e\left(\frac{-n^2\pi^2\alpha^2}{L^2}\right) \quad (30)$$

And

$$\mathrm{Dn} = \frac{2}{L}\int_0^L \mathrm{Cos}\left(2n + \frac{1}{2L\pi x}\right) dx \text{ because f(x) is 1 everywhere} \quad (31)$$

A.2 MATLAB Code to solve for Alpha:

```
clear all
clc
close all

r_f = 0.55;
alpha = .00027

x = linspace(0,20000);

y_exp = [0  0    0
0.437019372 0.463529042 0.154509681
0.16205112  0.16205112  0.176168141
0.195441005 0.201455977 0.201455977
0.234325533 0.2239058   0.239365368
0.239365368 0.249139374 0.27639532
0.27639532  0.27639532  0.289061144
0.297205305 0.297205305 0.301194817
0.312858259 0.309019362 0.316650618
0.312858259 0.309019362 0.324102241
0.327764529 0.334969006 0.33851375
0.334969006 0.33851375  0.355707998
0.352336282 0.348931987 0.36563664
0.362357321 0.36563664  0.378469878
0.375302711 0.372108587 0.387816221
0.381610761 0.372108587 0.393923939
0.396942557 0.393923939 0.411703794
0.411703794 0.396942557 0.425953795
0.417462169 0.417462169 0.437019372
0.428746964 0.431522054 0.442448392
0.431522054 0.431522054 0.450469258
0.439742261 0.434279412 0.458349784
0.445138073 0.434279412 0.46609709
0.458349784 0.455738083 0.471191199
0.458349784 0.458349784 0.47623082
0.46609709  0.468651066 0.481217666
0.471191199 0.471191199 0.488602512
0.481217666 0.478730736 0.493464348
0.488602512 0.491039447 0.503047075
0.495877391 0.493464348 0.507770625
0.495877391 0.498278749 0.512450638
0.498278749 0.500668588 0.512450638
0.500668588 0.500668588 0.519391595
0.500668588 0.503047075 0.521684725
0.505414368 0.507770625 0.52624101
0.505414368 0.507770625 0.530758183
0.510115999 0.510115999 0.535237235
0.517088295 0.512450638 0.537462763
0.519391595 0.521684725 0.537462763
0.52396782  0.530758183 0.546274215
0.537462763 0.530758183 0.548454959
0.539679114 0.537462763 0.552790639
0.546274215 0.544084731 0.557092577
0.546274215 0.548454959 0.561361548
```

```
0.5418864   0.546274215 0.557092577];

x_exp = [0
5
10
15
20
25
30
35
40
45
50
55
60
65
70
75
80
85
90
95
100
105
110
115
120
125
130
135
140
145
150
155
160
165
170
175
180
185
190
195
200
205
210
215
300];

y_mod = r_f*(1-exp(-alpha.*x));

figure
hold on
plot(x,y_mod);
plot(x_exp*60,y_exp(:,1),'*');
```

A 3. MATLAB Code of Model of Hydrogel:

```
% ******************************************************************
% *****                Hydrogel Elongation                    *****
% ******************************************************************

% Analytically obtain the hydrogel elongation for water collection project


% ------------------------------------
clear all
clc
close all;
% ------------------------------------

% +++++++++++++++++++++++
%    Input Parameters
% +++++++++++++++++++++++

%--- Compression Test----
clear all
clc
close all



A_0 = 675E-6;                    %| Initial area of the compressed object (m^2)
h_0 = 27E-3;                     %| Initial height of the compressed object (m)
h_c = 24.3E-3;                   %| The height of the compressed object (m)
w = 23.46;                       %| Weight (g)


w = w/1000*9.81;                 %| Weight (N)

%--- Free Swelling Test ---
d_u = 3;                     %| Dry diameter (mm)
d_s = 10;                    %| Swollen diameter (mm)
lambda_s = (d_s/d_u)^(1);
%

t_max = 20000;                 %| Maximum time of interest (s)


%----------------- Hydrogel Parameters ----------------%

k_b = 1.38E-23;
R = 8.2144598;               %| Gas Constant
T = 293;                     %| Temperature (K)
nu = 1E-3;
phi_0 = 1;                   %| Initial Volume Fraction
r = 0.005;                     %| Radius of hydrogel (m)

alpha = 4.3E-10;                   %| Permeability (m^2/s)


RT = R*T;
```

```matlab
kbT = k_b*T;
%-------------------------------------------------------%

%-- Finding the Shear Modulus

P_zz = w/A_0; % Nominal Stress
lambda_z = h_c/h_0;

G = -P_zz/(lambda_z-1/lambda_z^2); % This is computed using Neo-Hookean material

ro_x = G/RT;

%-- Finding the chi parameter

% lambda_s = (V/V_0)^(1/3);

% chi = -G/RT*kbT/2*lambda_s^5-kbT/n*(lambda_s^6*log(1-1/lambda_s^3)+lambda_s^3)*1E17;

chi = -G/RT*nu*(lambda_s^5-lambda_s^3)-lambda_s^6*log(1-1/lambda_s^3)-lambda_s^3;



%----- Diffusion Model -----%

n = 1; % Order of Bessel series

lambda = [2.405, 5.20, 8.654, 11.79]; % Eigenvalues

t = linspace(0,t_max);

phi = zeros(1,length(t));

for i = 1:length(t)
    for j = 1:n
        phi(i) = phi(i) + 2/1.6*phi_0*besselj(0,0)/(lambda(j)*besselj(1,lambda(j)))*exp(-
alpha*lambda(j)^2/r^2*t(i));
    end
end

elong = 1./phi;

figure(1)
hold on

plot(t,elong*.003*1.27,'k','linewidth',2)
xlabel('t (s)')
ylabel('\lambda')
```